

A Simplified Model Predictive Control for Shunt Active Power Filter Using Modified Instantaneous Power Theory under Polluted Grid Conditions

Hocine Bouchikha¹, Nadhir Mesbahi^{2*}✉, Larouci Heguig³, Ahmed Ouari¹

¹Department of Electrical Engineering, Faculty of Sciences Engineering, Badji-Mokhtar- Annaba University, P.O. Box 12, 23000, Annaba, Algeria

²Laboratoire de Génie Electrique et des Energies Renouvelables d'El Oued (LGEERE), Department of Electrical Engineering, Faculty of Technology, University of El Oued, 39000 El Oued, Algeria

³Institute of Science, Nour Bachir University Center - El Bayadh, Algeria

✉ nadhir-mesbahi@univ-eloued.dz

Abstract

This paper proposes a simplified finite control set model predictive control (FCS-MPC) strategy for a three-phase shunt active power filter (SAPF), which is based on a vector operation technique (VOT). In the conventional FCS-MPC, the optimal switching state is selected based on the evaluation and minimization of a cost function for all possible voltage vectors of the voltage source inverter (eight different vectors). The proposed FCS-MPC performs like a conventional FCS-MPC where the selection and evaluation of the possible voltage vectors are reduced by half (four vectors). The reduction in the computational burden is evident. In this study, the modified version of the instantaneous power theory based on a high selectivity filter is used to extract reference current components which increase the selectivity and the dynamic performance of SAPF. Simulation results demonstrate the effectiveness and reliability of the SAPF with the proposed control strategy under polluted grid conditions.

Keywords: Shunt Active Power Filter (SAPF), Model Predictive Control (MPC), High Selectivity Filter (HSF), Instantaneous Power (p-q) Theory, Non-Ideal Grid Voltages.

1 Introduction

The main cause of current harmonics generation is the use of extensive applications of nonlinear loads connected to the utility grid, such as rectifiers, computer power, electronic lighting, air-conditioning systems and variable frequency drives. Consequently,

the power quality of the distribution system deteriorates, especially the power factor of an operating power system [1]. To mitigate these harmonics, shunt active power filters (SAPFs) present an alternative solution to conventional passive filters for power quality problems. To ensure sinusoidal form at the point of common coupling (PCC), the SAPF injects compensating currents equal in magnitude and opposite in phase to harmonic currents [2-4].

Basically, the performances of the SAPF depend on the extraction method used to generate the reference current algorithm.

Moreover, the SAPF current control is employed to generate the switching pulses for voltage source inverter (VSI). The role of the harmonics extraction method is important in order to ensure appropriate injection current from SAPF[5].

A number of extraction methods under ideal grid voltage conditions have been reported in the literature such as the instantaneous power (p-q) theory algorithm [6], synchronous reference frame (SRF) [7] and fast Fourier transform (FFT) [8]. However, in real conditions, the grid voltages are most likely to be non-ideal (distorted and/or unbalanced). In this case, some extraction methods fail to correctly compute the reference current. To avoid the problem, a modified version of the instantaneous power theory method is presented in this paper for a three-phase shunt active power filter.

In this scheme high selectivity filters (HSF) have been selected instead of the classical extraction filters (low pass filters). With this method the total harmonic distortion (THD) of the grid currents is reduced, improving its quality [1,9].

In the literature, several current control methods for SAPF have been proposed in the past. They are hysteresis [10], repetitive [11], sliding mode control [12], optimal control and model predictive control (MPC) [13]. In comparison, predictive control schemes can provide better dynamic response with high accurate current control in a transient state. In addition, control can be directly applied to the SAPF without needing an external modulator[14].

Model predictive control can be classified into three categories: 1) Continuous-control-set model predictive control (CCS-MPC) or 2) finite-control-set model predictive control (FCS-MPC) and 3) deadbeat predictive control [15]. To implement FCS-MPC it is necessary to obtain a discrete time model of the SAPF. Its characterized by a limited number of switching states, to predict future behavior of the SAPF current in each sampling period. However, the main disadvantage is its high calculation burden.

The vector operation technique (VOT) can be used to reduce the calculation burden. This technique has the advantage that only two phase-legs are switching at high frequency, reducing the switching losses and also avoiding cross-coupling between controllers [16, 17]. The principle of VOT is that, for each sector, the number of possible voltage vectors to be considered can be reduced by half. Furthermore, in each sector, only two phase-legs are switching at high frequency while the remaining phase-leg is maintained at a constant DC-voltage value during this interval.

In contrast to other publications[16,17], this work presents a control for a three-phase SAPF using FCS-MPC with vector operation technique and a modified (p-q) method for computing reference current. This paper is organized as follows. Section 2 presents a model of the SAPF system. Section 3 describes the algorithm of FSC-MPC with VOT in $(\alpha - \beta)$ frame considering the discrete-time mathematical model of the three-phase SAPF system. Section 4 details the modified (p-q) scheme for generating the current

reference. Then, the results of the simulation investigations in various cases are given in Section 5 and the conclusion is summarized in Section 6.

2 Modeling of three-phase SAPF

The circuit configuration of the proposed three-phase SAPF model is illustrated in Figure 1. The SAPF is connected at the point of common coupling between the three-phase grid and nonlinear load. A three-phase diode bridge rectifier, feeding series connected R and L elements, is used as nonlinear load.

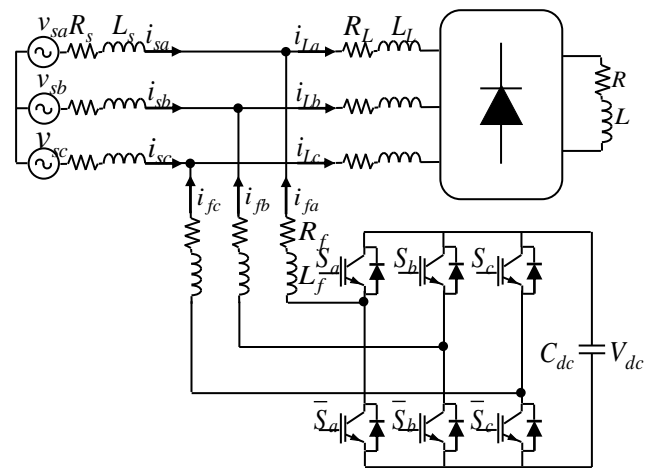


Figure 1: Main topology of three-phase two-level SAPF

The grid voltages and current are denoted as v_s and i_s respectively. Grid impedance is modeled as the connection of R_s and L_s . i_{La} , i_{Lb} and i_{Lc} represent the load currents, and the compensating currents injected by the SAPF are labelled as i_{fa} , i_{fb} and i_{fc} . C is the capacitance of the voltage source inverter DC-side capacitor.

According to the Kirchhoff law, the mathematical model of the SAPF in the (abc) frame can be expressed as:

$$L_f \frac{di_{fa}}{dt} + R_f i_{fa} = v_{fa} - v_{sa} \quad (1)$$



$$L_f \frac{di_{fb}}{dt} + R_f i_{fb} = v_{fb} - v_{sb} \quad (2)$$

$$L_f \frac{di_{fc}}{dt} + R_f i_{fc} = v_{fc} - v_{sc} \quad (3)$$

$$L_f \frac{di_{f\alpha}}{dt} + R_f i_{f\alpha} = v_{f\alpha} - v_{s\alpha} \quad (5)$$

$$L_f \frac{di_{f\beta}}{dt} + R_f i_{f\beta} = v_{f\beta} - v_{s\beta} \quad (6)$$

The space voltage vector of SAPF structure is defined as:

$$v_f = \frac{2}{3}(v_{fa} + av_{fb} + a^2v_{fc}) \quad (4)$$

where $a = e^{j(2\pi/3)}$ is the rotation factor.

Considering all possible combinations of the gating signals S_a , S_b , and S_c , eight voltage vectors are obtained, as shown in Table 1. Note that V_0 and V_7 are zero voltage vectors.

Table 1: Switching states and voltage vectors

S_a	S_b	S_c	v_f
0	0	0	$V_0 = 0$
1	0	0	$V_1 = \frac{2}{3}V_{dc}$
1	1	0	$V_2 = \frac{1}{3}V_{dc} + j\frac{\sqrt{3}}{3}V_{dc}$
0	1	0	$V_3 = -\frac{1}{3}V_{dc} + j\frac{\sqrt{3}}{3}V_{dc}$
0	1	1	$V_4 = -\frac{2}{3}V_{dc}$
0	0	1	$V_5 = -\frac{1}{3}V_{dc} - j\frac{\sqrt{3}}{3}V_{dc}$
1	0	1	$V_6 = \frac{1}{3}V_{dc} - j\frac{\sqrt{3}}{3}V_{dc}$
1	1	1	$V_7 = 0$

The mathematical model dynamics are then represented in the $(\alpha - \beta)$ orthogonal coordinates as:

3 Finite control set model predictive current control

The finite control set MPC involves two main steps: 1) predicting control variables for all admissible switching states of the inverter; and 2) evaluating the predicted values in a cost function and determining the state that minimizes the cost function. The cost function is composed of the errors between references and predicted control variables. This work considers a cost function for SAPF current control [18].

3.1. Discrete-time predictive model

The discrete-time model of the SAPF current dynamics for a sampling time T_s represents the predictive model. It will be used to predict the future value of SAPF currents considering all voltage vectors. Considering α -phase current, one may approximate its changing rate by:

$$\frac{di_{fa}}{dt} \approx \frac{i_{fa}(k+1) - i_{fa}(k)}{T_s} \quad (7)$$

where $i_{fa}(k+1)$ and $i_{fa}(k)$ are the sampled currents at the $k+1$ and k instants, respectively. The predicted filter current at the next sampling instant, which is calculated by discretizing (1), is given by the following:

$$L_f \left(\frac{i_{fa}(k+1) - i_{fa}(k)}{T_s} \right) + R_f i_{fa}(k) = v_{fa}(k) - v_{sa}(k) \quad (8)$$

Simplify (8), the predictive current at $k+1$ instant is given as follows:



$$i_{fa}(k+1) = \frac{T_s}{L_f} (v_{fa}(k) - v_{sa}(k)) + \left(1 - \frac{R_f T_s}{L_f}\right) i_{fa}(k) \quad (9)$$

3.2. Conventional FCS-MPC

The main control objective of current predictive control is to track reference current. The cost function of the current predictive control can be defined as:

$$g = \left| i_{f\alpha}^*(k+1) - i_{f\alpha}^p(k+1) \right| + \left| i_{f\beta}^*(k+1) - i_{f\beta}^p(k+1) \right| \quad (10)$$

where $i_{f\alpha}^p(k+1)$ and $i_{f\beta}^p(k+1)$ are the real and imaginary components of the predicted SAPF current which are obtained by using the system model; $i_{f\alpha}^*(k+1)$ and $i_{f\beta}^*(k+1)$ are the real and imaginary components of the reference current which will be explained in detail in the following section.

During each sampling period, the switching state that generates the minimum value of g is selected from eight possible function values. In other words, a conventional FCS-MPC of SAPF requires eight calculations and evaluation for all these eight voltage vectors. These calculations are computationally expensive and need powerful hardware.

3.3. Proposed FCS-MPC with VOT

One of the major drawbacks in conventional FCS-MPC is the evaluation of all possible voltage vectors of the VSI, which lead to a high computational burden and limits the sampling frequency. To overcome this problem a simplified FS-MPC has been introduced in [16, 17]. In the proposed strategy, the number of possible voltage vectors can be reduced to four, as it will be shown latter. Therefore, the computational load of the control algorithm will be clearly reduced. To explain vector selection based on the vector operation technique, the whole $(\alpha - \beta)$ plane is divided into six sectors, as shown in Figure 2.

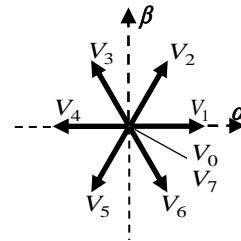


Figure 2: Voltage vectors in the complex plane

According to the sign of the grid voltages (positive or negative), the selection of four possible voltage vectors in each sector are chosen. As shown in Figure 3, for sector 1 ($0^\circ - 60^\circ$) the voltages v_{sa} and v_{sc} have the same sign, and consequently the high frequency phase-legs are a and c . As a consequence, the inactive phase leg will be phase-leg

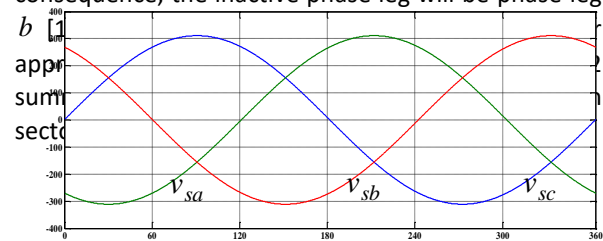


Figure 3: Three-phase grid voltages and sixty degrees sectors

Table 2: Pre-selection voltage vectors for each sector

Sector	v_{sa}	v_{sb}	v_{sc}	S_a	S_b	S_c	v_f
$0^\circ - 60^\circ$	+	-	+	X	0	X	V_0, V_1, V_5, V_6
$60^\circ - 120^\circ$	+	-	-	1	X	X	V_1, V_2, V_6, V_7
$120^\circ - 180^\circ$	+	+	-	X	X	0	V_0, V_1, V_2, V_3
$180^\circ - 240^\circ$	-	+	-	X	1	X	V_2, V_3, V_4, V_7
$240^\circ - 300^\circ$	-	+	+	0	X	X	V_0, V_3, V_4, V_5
$300^\circ - 360^\circ$	-	-	+	X	X	1	V_4, V_5, V_6, V_7

Finally, the objective of the proposed FCS-MPC with VOT can be obtained by evaluating the cost function for all sectors. The overall control system is illustrated in Figure 4.

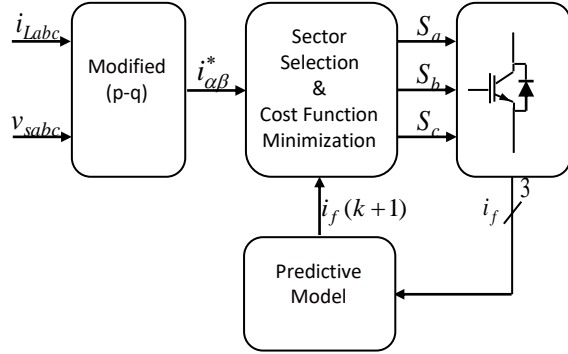


Figure 4: Control block diagram of FCS-MPC with VOT for SAPF

4 Reference current generation

In this paper, the reference current signal is derived from the measured quantities by using the modified instantaneous power theory. The main steps of this method are summarized in the diagram of Figure 5. In this scheme, the Concordia transformation can be expressed for a three phase system (nonlinear load current and grid voltage) as follows:

$$\begin{bmatrix} i_{L\alpha} \\ i_{L\beta} \end{bmatrix} = \sqrt{\frac{2}{3}} \begin{bmatrix} 1 & -\frac{1}{2} & -\frac{1}{2} \\ 0 & \frac{\sqrt{3}}{2} & -\frac{\sqrt{3}}{2} \end{bmatrix} \begin{bmatrix} i_{La} \\ i_{Lb} \\ i_{Lc} \end{bmatrix} \quad (11)$$

$$\begin{bmatrix} v_{s\alpha} \\ v_{s\beta} \end{bmatrix} = \sqrt{\frac{2}{3}} \begin{bmatrix} 1 & -\frac{1}{2} & -\frac{1}{2} \\ 0 & \frac{\sqrt{3}}{2} & -\frac{\sqrt{3}}{2} \end{bmatrix} \begin{bmatrix} v_{sa} \\ v_{sb} \\ v_{sc} \end{bmatrix} \quad (12)$$

Therefore, the load currents in $(\alpha - \beta)$ axis can also be decomposed into (dc) and (ac) components as follows:

$$\begin{cases} i_{L\alpha} = i_{L\alpha(dc)} + i_{L\alpha(ac)} \\ i_{L\beta} = i_{L\beta(dc)} + i_{L\beta(ac)} \end{cases} \quad (13)$$

Then, the high selectivity filter extracts the fundamental components directly from the currents in the $(\alpha - \beta)$ axis. After that, the $(\alpha - \beta)$ harmonic components of the load currents are computed by subtracting the HSF input signals from the corresponding outputs.

This approach can be expressed as follows [19, 20]:

$$\begin{bmatrix} i_{L\alpha(dc)}(s) \\ i_{L\beta(dc)}(s) \\ -i_{L\beta(dc)}(s) \\ i_{L\alpha(dc)}(s) \end{bmatrix} = \frac{K}{s} \begin{bmatrix} i_{L\alpha}(s) - i_{L\alpha(dc)}(s) \\ i_{L\beta}(s) - i_{L\beta(dc)}(s) \end{bmatrix} + \frac{2\pi f_c}{s} \quad (14)$$

where K is a constant gain parameter and f_c is the cutoff frequency.

On the other hand, under non-ideal conditions, grid voltage in $(\alpha - \beta)$ frame can actually be decomposed into (dc) and (ac) components as follows:

$$\begin{cases} v_{s\alpha} = v_{s\alpha(dc)} + v_{s\alpha(ac)} \\ v_{s\beta} = v_{s\beta(dc)} + v_{s\beta(ac)} \end{cases} \quad (15)$$

The transfer function of HSF for grid voltage can be summarized as follows:

$$\begin{bmatrix} v_{s\alpha(dc)}(s) \\ v_{s\beta(dc)}(s) \end{bmatrix} = \frac{K}{s} \begin{bmatrix} v_{s\alpha}(s) - v_{s\alpha(dc)}(s) \\ v_{s\beta}(s) - v_{s\beta(dc)}(s) \end{bmatrix} + \frac{2\pi f_c}{s} \begin{bmatrix} -v_{s\beta(dc)}(s) \\ v_{s\alpha(dc)}(s) \end{bmatrix} \quad (16)$$

The instantaneous active and reactive power is represented as follows:

$$\begin{bmatrix} P_{(ac)} \\ q_{(ac)} \end{bmatrix} = \begin{bmatrix} v_{s\alpha(dc)} & v_{s\beta(dc)} \\ -v_{s\beta(dc)} & v_{s\alpha(dc)} \end{bmatrix} \begin{bmatrix} i_{L\alpha(ac)} \\ i_{L\beta(ac)} \end{bmatrix} \quad (17)$$

where $p_{(ac)}$ and $q_{(ac)}$ represent the distorted (ac) components of instantaneous real and imaginary powers, respectively.

Therefore, the reference currents in the $(\alpha - \beta)$ frame are obtained by:

$$\begin{bmatrix} i_{\alpha}^* \\ i_{\beta}^* \end{bmatrix} = \frac{1}{v_{s\alpha(dc)}^2 + v_{s\beta(dc)}^2} \begin{bmatrix} v_{s\alpha(dc)} & -v_{s\beta(dc)} \\ v_{s\beta(dc)} & v_{s\alpha(dc)} \end{bmatrix} \begin{bmatrix} P_{(ac)} + P_c \\ q \end{bmatrix} \quad (18)$$

where p_c is an active power required for regulating DC bus voltage.

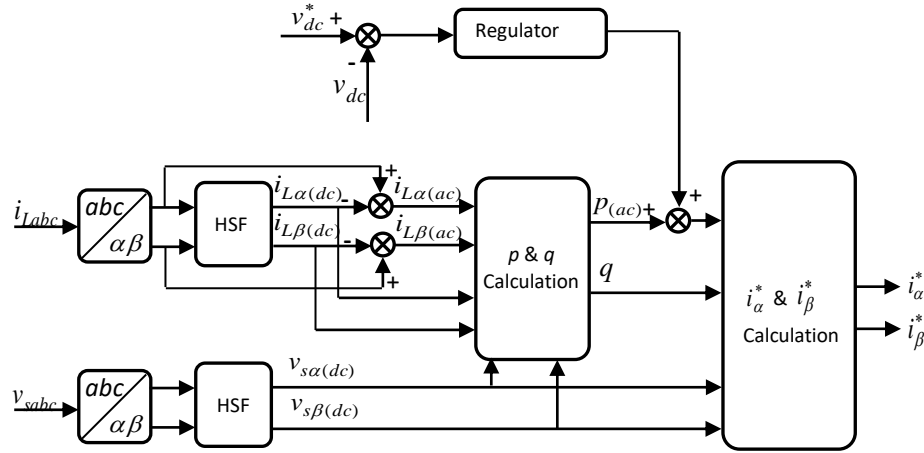


Figure 5: Block diagram of modified (p-q) theory

5 Simulation results and analysis

Simulations are carried out in Matlab/Simulink software and the proposed FCS-MPC strategy is implemented and evaluated. The main purpose of the simulation is to test control law performance under the following four different aspects: 1) steady-state performance of the SAPF under the balanced condition of the grid voltages; 2) performance of the SAPF under the unbalanced condition of the grid voltages; 3) performance of the SAPF under the distorted condition of the grid voltages; and 4) performance of the SAPF during load change. The main system parameters are presented in Table 3.

Table 3: Design specifications of SAPF

Parameter	Value
Grid voltage	220 V
Grid resistor	0.1 Ω
Grid inductance	0.5 mH
Grid frequency	50 Hz
Load AC resistor	1.2 m Ω
Load AC inductance	0.3 mH
DC voltage	800 V
DC capacitor	3300 μ F
Filter resistor	5 m Ω
Filter inductance	5 mH
Load resistor	40 Ω
Load inductor	50 mH
Sampling frequency	40 kHz

5.1 Steady-state performance of the SAPF under the balanced condition of the grid voltages

Figure 6 shows the main SAPF waveforms of the proposed method when the grid voltage is sinusoidal and balanced. The grid voltages (v_{sabc}), load currents (i_{Labc}), grid currents (i_{sabc}) and filter currents (i_{fabc}) are depicted there.

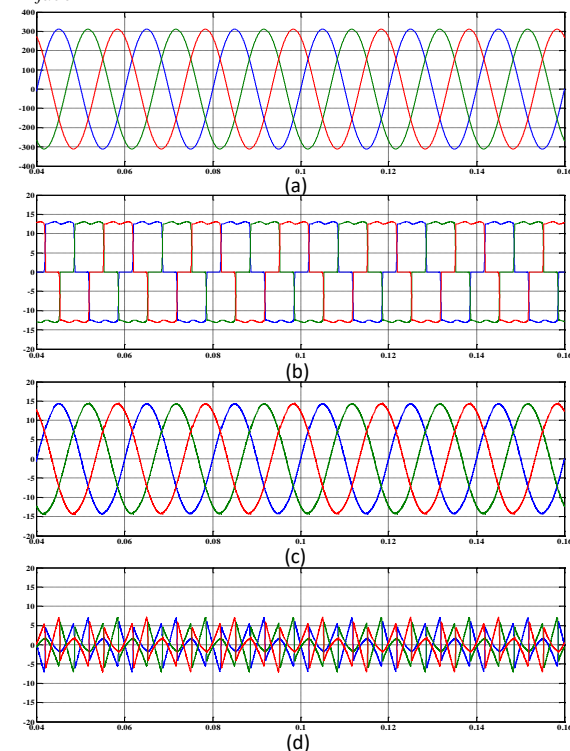


Figure 6: Simulation results of SAPF under balanced sinusoidal grid voltage: (a) three-phase grid voltages, (b) load currents, (c) grid currents, (d) filter currents

It can be seen from the waveform of the load current that its harmonic content is high. After compensation, the waveform of the grid current is approximately sinusoidal and in phase with the grid voltage.

Figure 7 illustrates the harmonic spectrum of the grid current before and after filtering. It confirms that the proposed FCS-MPC compensates the total harmonic distortion of the grid current. The THD of the grid current was reduced from 28.80% before compensation to 1.52% after compensation. Further, the DC-link voltage is maintained at its reference value of 800 V, as shown in Figure 8.

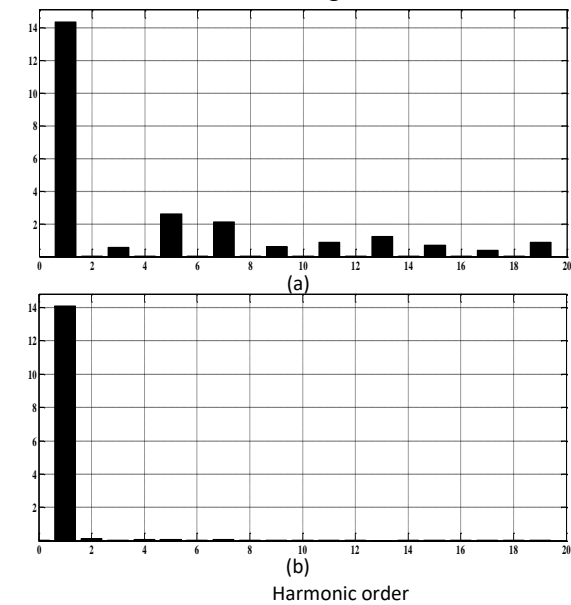


Figure 7: Harmonic spectrum of phase-a grid current: (a) before compensation, (b) after compensation

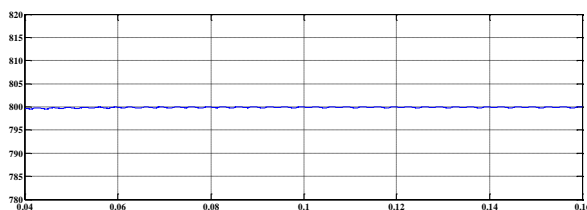


Figure 8: DC-link voltage

5.2 Performance of the SAPF under the unbalanced condition of the grid voltages

Figure 9 shows the main SAPF waveforms when the grid voltage is sinusoidal but unbalanced. The RMS values of each phase of the grid voltage are 240V, 220V and 200V respectively.

The proposed method can still make the grid current sinusoidal and balanced. The THD of the grid currents

(i_{sabc}) before compensation are respectively 26.42%, 29.41% and 30.88% while after compensation they are 1.56%, 1.61% and 1.70%. The DC-link voltage is also stable and it is maintained near its desired regulated value of 800 V.

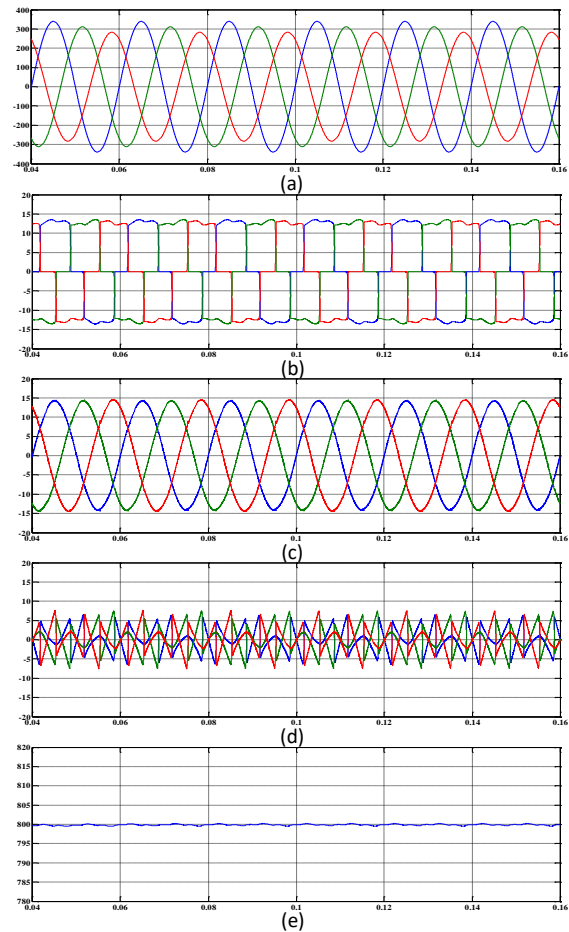


Figure 9: Simulation results of SAPF under unbalanced sinusoidal grid voltage: (a) three-phase grid voltages, (b) load currents, (c) grid currents, (d) filter currents, (e) DC-link voltage

5.3 Performance of the SAPF under the distorted condition of the grid voltages

Figure 10 shows the behavior of the SAPF under non-sinusoidal voltage grid condition. In this case the grid voltage is not sinusoidal and includes a 7th harmonic component (THDv= 14.29%). The THD of the grid current under this condition is 3.24% after filtering. The simulation results verify the effectiveness and performances of the proposed method under distorted grid voltages. Notice that the grid currents

after compensation are almost sinusoidal and balanced.

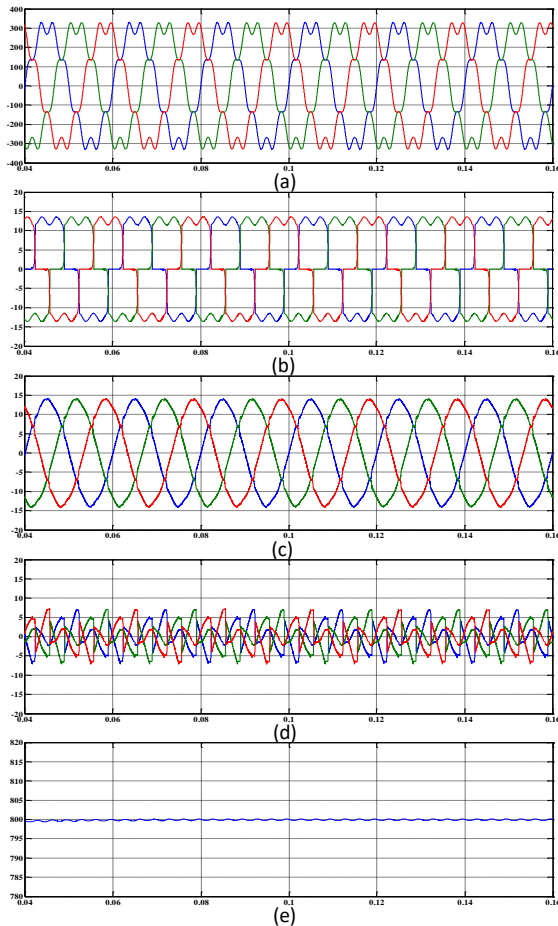


Figure 10: Simulation results of SAPF under distorted sinusoidal grid voltage: (a) three-phase grid voltages, (b) load currents, (c) grid currents, (d) filter currents, (e) DC-link voltage

5.4 Performance of the SAPF during load change

To study the dynamic performance of the proposed FCS-MPC with VOT, the system has been simulated under a 100% step change in the load current. The Figure 11 shows the simulation results under dynamic load conditions. These waveforms show the dynamic capability of SAPF to compensate harmonic currents of the load under this sudden variation in the load.

Based on all the results obtained from numerical simulations, it is shown that the proposed FCS-MPC confirms that the grid current is almost sinusoidal and balanced after compensation.

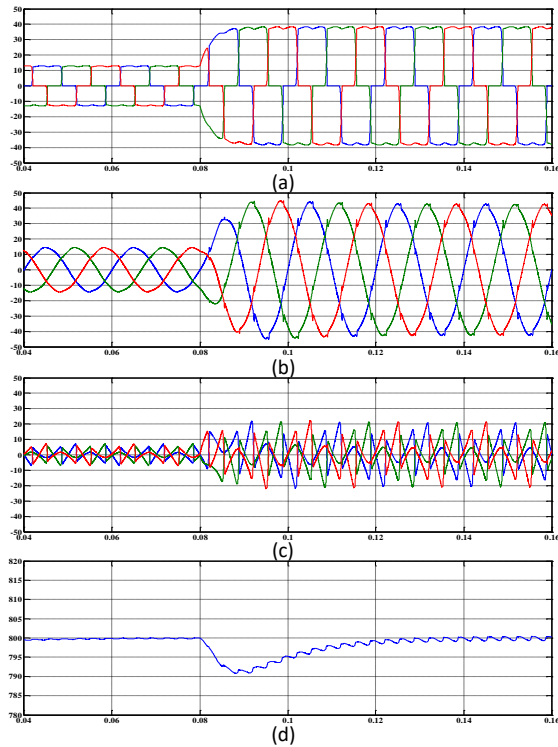


Figure 11: Performance of SAPF during load change: (a) load currents, (b) grid currents, (c) filter currents, (d) DC-link voltage

6 Conclusion

This paper presents an FCS-MPC strategy for a three-phase shunt active power filter with vector operation technique. The FCS-MPC with VOT approach is introduced to select the optimal vector, which requires only four voltage vectors to be predicted instead of all of the voltage vectors. As a result, the computation time of the proposed method is significantly reduced, compared to the traditional FCS-MPC strategy. The effectiveness of the proposed method was validated using Matlab/Simulink software. The simulation results demonstrate the effectiveness of the proposed control algorithm for various operating conditions, such as unbalanced or distorted grid voltages.

References

- [1] Mesbahi N, Ouari A, Ould Abdeslam D, Djama T, Omeiri A. Direct power control of shunt active



- filter using high selectivity filter (HSF) under distorted or unbalanced conditions. *Electric Power Systems Research* 2014; 108:113–123.
- [2] Singh B, Al-Haddad K, Chandra A. A review of active filters for power quality improvement. *IEEE Transactions on Industrial Electronics* 1999; 46: 960–971.
- [3] Mesbahi N, Ouari A, Omeiri A. Reference current computation for three-level shunt active filter under distorted and unbalanced conditions. In: *International Renewable and Sustainable Energy Conference (IRSEC)* 2013.
- [4] Guzman R, Garcia de Vicuna L, Morales J, Castilla M, Miret J. Model-based control for a three-phase shunt active power filter. *IEEE Transactions on Industrial Electronics* 2016; 63:3998–4007.
- [5] Isabel Milans M, Romero Cadaval E, Barrero Gonzalez F. Comparison of control strategies for shunt active power filters in three-phase four-wire systems. *IEEE Transactions on Power Electronics* 2007; 22: 229–236.
- [6] Popescu M, Bitoleanu A, Suru V. A DSP-based implementation of the p-q theory in active power filtering under nonideal voltage conditions. *IEEE Transactions on Industrial Informatics* 2013; 9:880–889.
- [7] Monfared M, Golestan S, Guerrero J.M. A new synchronous reference frame-based method for single-phase shunt active power filters. *Journal of Power Electronics* 2013; 13:692–700.
- [8] Vodyakho O, Mi C.C. Three-level inverter-based shunt active power filter in three-phase three-wire and four-wire systems. *IEEE Transactions on Power Electronics* 2009; 24:1350–1363.
- [9] Abdusalam M, Poure P, Karimi S, Saadate S. New digital reference current generation for shunt active power filter under distorted voltage conditions. *Electric Power Systems Research* 2009; 79:759–765.
- [10] Tey L.H, So P.L, Chu Y.C. Improvement of power quality using adaptive shunt active filter. *IEEE Transactions on Power Delivery* 2005; 20:1558–1568.
- [11] Ramos G.A, Costa-Castelló R. Power factor correction and harmonic compensation using second-order odd-harmonic repetitive control. *IET Control Theory Applications* 2012; 6:1633–1644.
- [12] Matas J, de Vicuna L.G, Miret J, Guerrero J.M, Castilla M. Feedback linearization of a single-phase active power filter via sliding mode control. *IEEE Transactions on Power Electronics* 2008; 23:116–125.
- [13] Acuña P, Morán L, Rivera M, Aguilera R, Burgos R, G. Agelidis V. A single-objective predictive control method for a multivariable single-phase three-level NPC converter-based active power filter. *IEEE Transactions on Industrial Electronics* 2015; 62:4598–4607.
- [14] Panigrahi R, Subudhi B, Panda P.C. Model predictive-based shunt active power filter with a new reference current estimation strategy. *IET Power Electronics* 2015; 8:221–233.
- [15] Abdelrahem M, M.Hackl C, Zhang Z, Kennel R. Robust predictive control for direct-driven surface-mounted permanent-magnet synchronous generators without mechanical sensors. *IEEE Transactions on Energy Conversion* 2018; 33:179–189.
- [16] Morales J, de Vicuna G.L, Guzman R, Castilla M, Miret J. Modeling and sliding mode control for three-phase active power filters using vector operation technique. *IEEE Transactions on Industrial Electronics* 2018; 65:6828–6838.
- [17] Guzman R, de Vicuna G.L, Castilla M, Miret J, Camacho A. Finite control set model predictive control for a three-phase shunt active power filter with a kalman filter-based estimation. *Energies* 2017; 10.
- [18] Rodríguez J, Pontt J, A.Silva C, Correa P, Lezana P, Cortés P, Ammann U. Predictive control of a voltage source inverter. *IEEE Transactions on Industrial Electronics* 2007; 54:495–503.
- [19] Ouari A, Mesbahi N, Omeiri A. High selectivity filter based reference current generation method for three-level shunt active power filters under adverse source voltage conditions. *International Journal of System Assurance Engineering and Management* 2014; 5:611–617.
- [20] Hoon Y, Amran Mohd Radzi M, Khair Hassan M, Farzilah Mailah N. Operation of three-level inverter-based shunt active power filter under non-ideal grid voltage conditions with dual fundamental component extraction. *IEEE Transactions on Power Electronics* 2018; 33:7558–7570.